



Deposited via The University of Sheffield.

White Rose Research Online URL for this paper:

<https://eprints.whiterose.ac.uk/id/eprint/191527/>

Version: Published Version

Article:

Prajsnar, T.K., Michno, B.J., Pooranachandran, N. et al. (2022) Phagosomal acidification Is required to kill *Streptococcus pneumoniae* in a Zebrafish model. *Cellular Microbiology*, 2022. 9429516. ISSN: 1462-5814

<https://doi.org/10.1155/2022/9429516>

Reuse

This article is distributed under the terms of the Creative Commons Attribution (CC BY) licence. This licence allows you to distribute, remix, tweak, and build upon the work, even commercially, as long as you credit the authors for the original work. More information and the full terms of the licence here:

<https://creativecommons.org/licenses/>

Takedown

If you consider content in White Rose Research Online to be in breach of UK law, please notify us by emailing eprints@whiterose.ac.uk including the URL of the record and the reason for the withdrawal request.

Research Article

Phagosomal Acidification Is Required to Kill *Streptococcus pneumoniae* in a Zebrafish Model

Tomasz K. Prajsnar ^{1,2} Bartosz J. Michno ² Niedharsan Pooranachandran ²
Andrew K. Fenton ³ Tim J. Mitchell,⁴ David H. Dockrell ⁵ and Stephen A. Renshaw ¹

¹Bateson Centre & Department of Infection, Immunity and Cardiovascular Disease, University of Sheffield, Sheffield, UK

²Department of Evolutionary Immunology, Institute of Zoology and Biomedical Research, Faculty of Biology, Jagiellonian University, Krakow, Poland

³The Florey Institute for Host-Pathogen Interactions, School of Biosciences, University of Sheffield, UK

⁴Institute of Microbiology and Infection, College of Medical and Dental Sciences, University of Birmingham, Birmingham, UK

⁵Department of Infection Medicine & Centre for Inflammation Research, University of Edinburgh, Edinburgh, UK

Correspondence should be addressed to Tomasz K. Prajsnar; tomasz.prajsnar@uj.edu.pl

Received 1 March 2022; Accepted 23 April 2022; Published 9 June 2022

Academic Editor: Roberto Botelho

Copyright © 2022 Tomasz K. Prajsnar et al. This is an open access article distributed under the Creative Commons Attribution License, which permits unrestricted use, distribution, and reproduction in any medium, provided the original work is properly cited.

Streptococcus pneumoniae (the pneumococcus) is a major human pathogen causing invasive disease, including community-acquired bacteraemia, and remains a leading cause of global mortality. Understanding the role of phagocytes in killing bacteria is still limited, especially *in vivo*. In this study, we established a zebrafish model to study the interaction between intravenously administered pneumococci and professional phagocytes such as macrophages and neutrophils, to unravel bacterial killing mechanisms employed by these immune cells. Our model confirmed the key role of polysaccharide capsule in promoting pneumococcal virulence through inhibition of phagocytosis. Conversely, we show pneumococci lacking a capsule are rapidly internalised by macrophages. Low doses of encapsulated *S. pneumoniae* cause near 100% mortality within 48 hours postinfection (hpi), while 50 times higher doses of unencapsulated pneumococci are easily cleared. Time course analysis of *in vivo* bacterial numbers reveals that while encapsulated pneumococcus proliferates to levels exceeding 10⁵ CFU at the time of host death, unencapsulated bacteria are unable to grow and are cleared within 20 hpi. Using genetically induced macrophage depletion, we confirmed an essential role for macrophages in bacterial clearance. Additionally, we show that upon phagocytosis by macrophages, phagosomes undergo rapid acidification. Genetic and chemical inhibition of vacuolar ATPase (v-ATPase) prevents intracellular bacterial killing and induces host death indicating a key role of phagosomal acidification in immunity to invading pneumococci. We also show that our model can be used to study the efficacy of antimicrobials against pneumococci *in vivo*. Collectively, our data confirm that larval zebrafish can be used to dissect killing mechanisms during pneumococcal infection *in vivo* and highlight key roles for phagosomal acidification in macrophages for pathogen clearance.

1. Introduction

Streptococcus pneumoniae is a major human pathogen causing a range of diseases including community-acquired pneumonia, meningitis, and bacteraemia. The mortality rates of invasive pneumococcal diseases can reach 30% [1]. The widespread use of antimicrobial therapies has contributed to antimicrobial resistance amongst pneumococci and serotype replacement is challenging vaccine efficacy [2].

S. pneumoniae has been long considered to be a classical extracellular pathogen where macrophages are key effectors of antibacterial host defence [3]. Of major importance to the pneumococcus is the polysaccharide capsule which promotes resistance to phagocytosis and allows extracellular proliferation [4]. It has been described *in vitro* that pneumococcal capsule protects against macrophage and neutrophil phagocytosis predominantly via inhibition of opsonisation with antibody and complement [5–9]. However, it has been

recently demonstrated that intracellular replication of pneumococcus occurs inside splenic macrophages serving as a reservoir for septicaemia [10]. It has also been postulated that intracellular pneumococci contribute to blood-brain barrier penetration via transcytosis which subsequently leads to meningitis [11].

It is generally accepted that professional phagocytes use a combination of oxidative and nonoxidative methods to kill bacterial cells [12]. Oxidative mechanisms rely on production of reactive species containing either oxygen (ROS) or nitrogen (RNS) and are generated by NADPH oxidase and mitochondria or nitric oxide synthases [3]. However, it has been shown experimentally that *S. pneumoniae* are relatively resistant to oxygen-dependent bacterial killing in a mouse model of pneumococcal pneumonia [13] and that ROS needs to combine with other factors to enable killing [14]. Many nonoxidative mechanisms of bacterial killing require acidification of phagosomes which is further aided by their later fusion with lysosomes. Phagosome acidification occurs through the action of the vacuolar ATPase (v-ATPase) which acts as a unidirectional proton pump thereby acidifying the phagosome [15–17]. The contribution of these bacterial killing approaches to pneumococcal clearance is not well understood. In addition, most phagocyte-pneumococcus interaction studies have been performed *in vitro* lacking the wider context of immune biology. To understand pneumococcal pathology, it is important to determine the mechanisms of pneumococcal killing by the innate immune system, especially *in vivo* where it is possible to study relative contributions of different kind of phagocytes and the mechanisms they use. Such understanding might support immunomodulatory therapeutic strategies as effective alternatives to antibiotics which would also help to reduce our reliance on vaccines [18].

Zebrafish have proven to be an excellent *in vivo* model to study host-pathogen interaction at molecular, cellular, and populational level [19]. Larval zebrafish have been successfully used to model systemic pneumococcal infection [20] as well as meningitis caused by pneumococci [21]. Although the roles of specific phagocyte killing mechanisms have not been determined, these studies demonstrated that zebrafish could serve as an alternative model of pneumococcal infection to increase our understanding of pneumococcal pathogenesis. In addition, infections caused by other streptococcal species have also been studied using zebrafish [22].

Here, using a larval zebrafish model of systemic *S. pneumoniae* infection, we show that unencapsulated pneumococci are rapidly ingested by mononuclear phagocytes, generally referred to as macrophages, and are efficiently killed following rapid acidification of phagosomes. We also demonstrate that this acidification of phagosomes containing bacteria is crucial for effective clearance of pneumococci and survival of the infected host.

2. Results

2.1. Pneumococcal Capsule Is Necessary for Virulence in a Zebrafish Larval Model. In order to induce systemic infection, we injected a range of doses of pneumococci into the

circulation of 54 h postfertilisation (hpf) London wild-type (LWT) zebrafish larvae. We analysed the virulence of a serotype 2 strain D39 [23], which is extensively used to study *S. pneumoniae* pathogenesis. The infected larvae were maintained at 28.2°C, and the survival of larvae was monitored up to 68 h post infection (hpi). Since the pneumococcal capsule has been considered a major virulence determinant important in immune evasion [1], we first examined its role in a larval zebrafish model of infection. We found that D39 and D39 Δcps strains displayed radically distinct virulence phenotypes (Figures 1(a) and 1(b)). Even low doses (approximately 40 CFU) of encapsulated D39 led to 100% mortality within 3 days (Figure 1(a)). Conversely, doses as high as 3000 CFU of unencapsulated D39 Δcps were unable to kill any infected larvae (Figure 1(b)). The striking differences between D39 and D39 Δcps prompted us to enumerate bacteria within larvae following infection. Infected larvae were homogenised and the numbers of bacteria within individual larvae determined. In larvae infected with D39, the number of bacteria increased exponentially, reaching approximately 10^5 CFU at 30 to 44 hpi, at which point death of some larvae occurred (Figure 1(c)). In contrast, strain D39 Δcps was unable to proliferate *in vivo* and bacterial numbers dramatically decreased, falling below the limit of detection by 20 hpi (Figure 1(d)). Thanks to the optical transparency of zebrafish larvae, we were able to follow these infections using GFP-tagged pneumococcal strains [9, 24]. Comparing infections between GFP-tagged D39 and D39 Δcps strains showed that at 24 hpi, high intensity of D39-GFP signal could be detected within zebrafish vasculature (Figure 1(e)). In contrast, the GFP-tagged D39 Δcps infected larvae were able to prevent bacterial *in vivo* growth within the larval vascular system (Figure 1(f)).

These results validated our larval zebrafish model and confirmed the model could identify key virulence determinants. Our data confirm the importance of pneumococcal capsule in disease progression of systemic infection and, in view of the well-established role of capsule in inhibiting phagocytosis [4], suggested that effective innate immune responses and clearance of bacteria were a key factor in determining outcome.

2.2. Pneumococcal Infection in Zebrafish Larvae Can Be Cured with Antibiotics. Zebrafish have also been successfully used to conduct chemical screens for small molecules of various biological activities [25]. We therefore asked whether our infection model could be used as a potential screening platform for novel antipneumococcal compounds. As a proof of principle, larvae infected with D39 were immersed in various concentrations of penicillin G added to the medium at 1 hpi. We found a dose-dependent response, with a concentration of 1.25 $\mu\text{g/ml}$ able to prevent the death of all infected larvae (Figure S1A). Microscopic imaging of infected larvae treated with the curative dose (1.25 $\mu\text{g/ml}$) of penicillin G or nontreated controls revealed that survival is associated with clearance of bacteria observed in treated larvae at 24 hpi (Figure S1C). As expected, untreated infected larvae supported intravascular bacterial proliferation (Figure S1B).

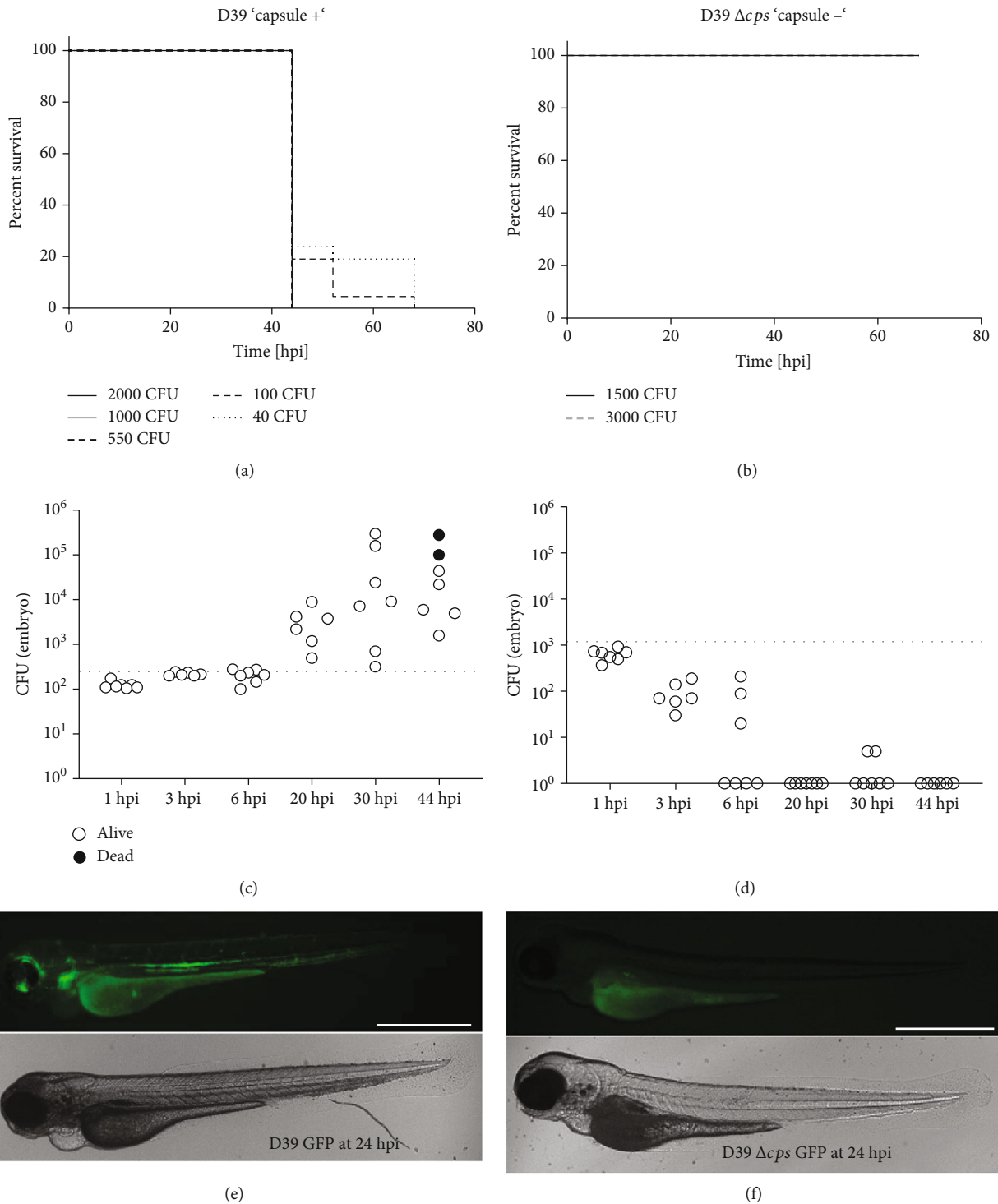


FIGURE 1: Encapsulated pneumococci kill zebrafish while unencapsulated pneumococci are rapidly cleared from infected larvae. (a–b) Survival of zebrafish larvae following infection at 54 hpf with indicated doses of encapsulated *S. pneumoniae* D39 WT (a) or unencapsulated *S. pneumoniae* D39 Δcps (b) monitored over 68 hpi ($n \geq 42$ individual animals over two independent experiments). (c–d) Numbers of viable colony forming units (CFUs) over time within zebrafish larvae ($n \geq 6$ per group per time point) infected with 100 CFU of encapsulated *S. pneumoniae* D39 (c) or 1500 CFU of unencapsulated *S. pneumoniae* D39 Δcps (d). Open circles represent living embryos, whereas solid circles show dead embryos at the time of sample collection. (e–f) Representative fluorescence (top) and brightfield (bottom) *in vivo* images ($n=10$) of zebrafish larvae at 24 hpi following injection with 100 CFU of GFP-labelled D39 (e) or 1500 CFU of D39 Δcps . Scale bars represent 500 μm .

We next decided to test the effect of treatment with a drug to which pneumococci are resistant. To this end, we used encapsulated strains, either sensitive (D39) or resistant (D39 GFP) to chloramphenicol. Again, as a proof of principle, we showed the ability to successfully treat susceptible (Figure S1D) but not resistant pneumococci (Figure S1E). Together, these data indicate that our model pneumococcal infection can be also used to screen for compounds that clear pathogens and potentially for novel antimicrobials and host-based therapies.

2.3. Systemically Administered Unencapsulated *Pneumococcus* Is Predominantly Internalised by Macrophages Whereas Its Encapsulated Counterpart Evades Phagocytosis. The dramatic difference in zebrafish survival and ability to clear the infection between encapsulated and unencapsulated pneumococcal strains aligned with knowledge of the inhibitory role of polysaccharide capsule on innate immune function, including phagocytosis [26]. This suggested the unencapsulated strain could be used to probe key innate immune responses associated with clearance. Nevertheless, the precise roles played by different phagocytes and the mechanisms they employ to clear pathogens remain elusive *in vivo* since environmental factors modulate function and limit translation from *in vitro* function [27]. Therefore, in order to determine the role of professional phagocytes (macrophages and neutrophils) in our systemic pneumococcal infection model, macrophage-labelled *Tg(mpeg1:mCherry-F)* larvae were infected with either encapsulated D39 GFP or unencapsulated D39 Δcps GFP and fixed at 1, 2, and 4 hpi and stained for neutrophils (by Cy5-TSA) for subsequent microscopic imaging (Figures 2(a) and 2(b), Figure S2, Figure S3). We found that the majority of encapsulated pneumococci remain free in the bloodstream whereas unencapsulated bacteria are readily internalised (Figure 2(c)). We also observed zebrafish macrophages were more likely to contain intracellular bacteria than neutrophils at all time points tested (Figures 2(d)–2(g)). Macrophages showed evidence of ingestion of bacteria at all time points from 1 to 4 hpi (Figures 2(f) and 2(g)). In the case of the encapsulated bacteria, only a minority were within macrophages and the majority of bacteria were extracellular (Figure 2(f)), while for the unencapsulated strain, the majority of bacteria were in macrophages or in the rare cases where they were not primarily in macrophages, they were located in neutrophils (Figure 2(g)). The shift to intracellular location with the unencapsulated strain also was associated with the clearance of this strain, while extracellular location of the encapsulated bacteria was associated with persistence of bacteria (Figures 2(h) and 2(i)). This corroborated our previous observation where total *in vivo* bacterial load was greater for encapsulated bacteria (Figures 1(c) and 1(d)). Together, these results confirm the key role of capsule in phagocyte evasion and the important contribution of macrophages in successful clearance of intravascular pneumococci *in vivo*.

2.4. Macrophages Are Critical in Clearance of *Pneumococci* in Zebrafish. Our *in vivo* imaging of zebrafish infected with fluorescent *S. pneumoniae* revealed that the majority of

unencapsulated pneumococci are phagocytosed by zebrafish macrophages. Therefore, to determine the importance of specific phagocytes in the immune defence to unencapsulated pneumococci, we depleted macrophages in the zebrafish larvae by knocking down *irf8*—a transcription factor responsible for macrophage development (Figure S4). In practice, the *irf8* knockdown in zebrafish results in the preferential development of neutrophils at the expense of macrophages [28] and it has been routinely used in several zebrafish infection studies [29–32]. This experiment revealed that macrophage-depleted larvae are highly susceptible to pneumococci and succumb to systemic infection with the unencapsulated strain within 2 days (Figure 3(a)). Interestingly, the determination of CFU counts within the macrophage-depleted larvae showed that unencapsulated pneumococci were now able to proliferate *in vivo* and overwhelmed the infected host, reaching nearly 10^5 CFU (Figure 3(b)) levels comparable to the encapsulated bacteria without macrophage depletion. Taken together, these data suggest that macrophages are critical for innate immunity to unencapsulated pneumococci and cannot be substituted by neutrophils.

2.5. Phagosomal Acidification within Macrophages Is Essential for Intracellular Killing of *Pneumococci*. We next addressed whether phagosome acidification and fusion with lysosomes could be important in pneumococcal killing upon phagocytosis by zebrafish macrophages observed in our infection model. To examine this, we treated the *S. pneumoniae*-infected larvae with bafilomycin A1—a potent v-ATPase inhibitor which also prevents fusion of phagosomes with lysosomes [33].

For these experiments, the transgenic larvae *Tg(fms:GFP)sh377* [34] were infected with D39 Δcps GFP which were prestained with the pH-sensitive dye pHrodo Red [35], which creates a higher fluorescence intensity at lower pH. We found that bacteria internalised by macrophages were acidified in control larvae and this acidification was inhibited by bafilomycin A1 in the medium (Figures 4(a)–4(c)). Importantly, the use of bafilomycin A1 did not block the internalisation of bacteria by macrophages and we did not observe any pronounced differences in number of bacterial per phagosome or phagosome types (Figure 4(b)). In addition, we noticed that the level of GFP fluorescence of internalised pneumococci was higher in the presence of bafilomycin A1. This is in line with previous studies reporting sensitivity of the GFP fluorescence intensity to low pH [36]. Lastly, we observed the degradation of bacteria within macrophages of control larvae and confirmed this degradation was inhibited in the presence of bafilomycin (Figures 4(d)–4(g)). We believe this observed suppression of acidification-mediated bacterial degradation would lead to intracellular survival of internalised pneumococci and promote disease progression.

Therefore, to determine the importance of phagosomal acidification in pneumococcal infection in zebrafish, 2 dpf larvae with either chemically or genetically inhibited v-ATPase were infected with unencapsulated D39 Δcps *S. pneumoniae*. For genetic inhibition, using CRISPR/Cas9,

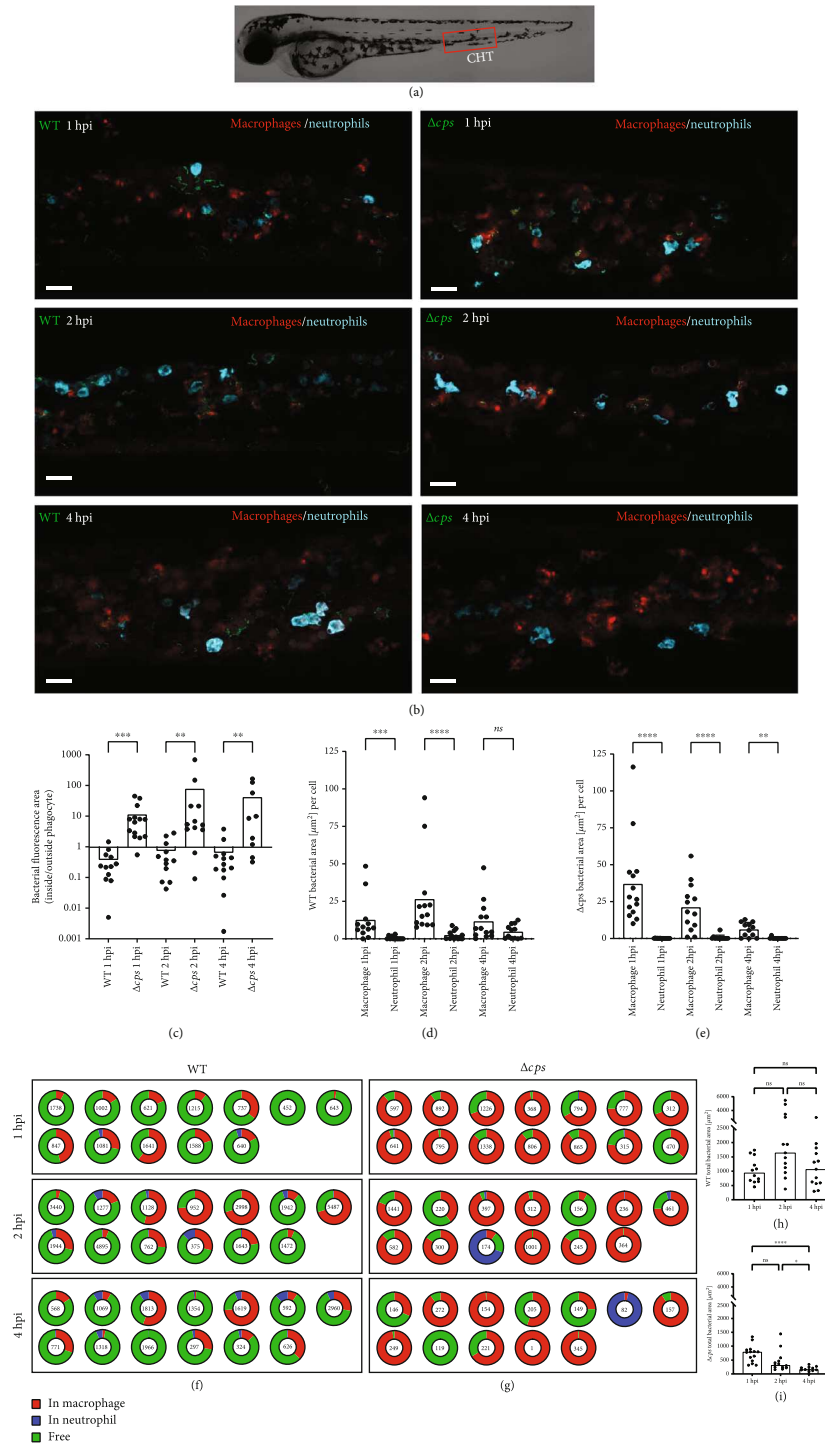


FIGURE 2: Unencapsulated pneumococci are rapidly internalised by zebrafish macrophages. (a–b) Representative images ($n=12-14$) of the caudal haematopoietic tissue (CHT, indicated by red rectangle in panel (a)) of *Tg(mpeg:mCherry-F)* transgenic larvae (red macrophages) fixed at 1, 2, and 4 hpi following injection with approximately 2000 CFU of D39WT GFP and D39 Δcps GFP strains. The larvae were stained with Cy5-TSA to visualise (blue) neutrophils. Scale bars represent 20 μm . (c) Quantification of internalisation rates of D39 WT GFP or D39 Δcps GFP by zebrafish phagocytes at 1, 2, and 4 hpi. The ratio of GFP fluorescence area outside to inside phagocytes was used to quantify bacterial uptake. (d–e) Quantification of D39 WT GFP (d) and D39 Δcps GFP (e) bacterial area within macrophages and neutrophils at each time point. (f–g) Pie charts showing the location of D39 WT GFP (f) and D39 Δcps GFP (g) *S. pneumoniae* cells in each imaged zebrafish larvae at each time point. Numbers inside rings indicate the total bacterial area within the image. (h–i) Quantification of total bacterial area within images of zebrafish larvae infected with D39 WT GFP (h) and D39 Δcps GFP (i) at each time point. Bar charts represent the mean with individual data points shown. 12–14 zebrafish larvae analysed in each time points and groups in two independent experiments. **** $p < 0.0001$, *** $p < 0.001$, ** $p < 0.01$, * $p < 0.05$, ns: not significant.

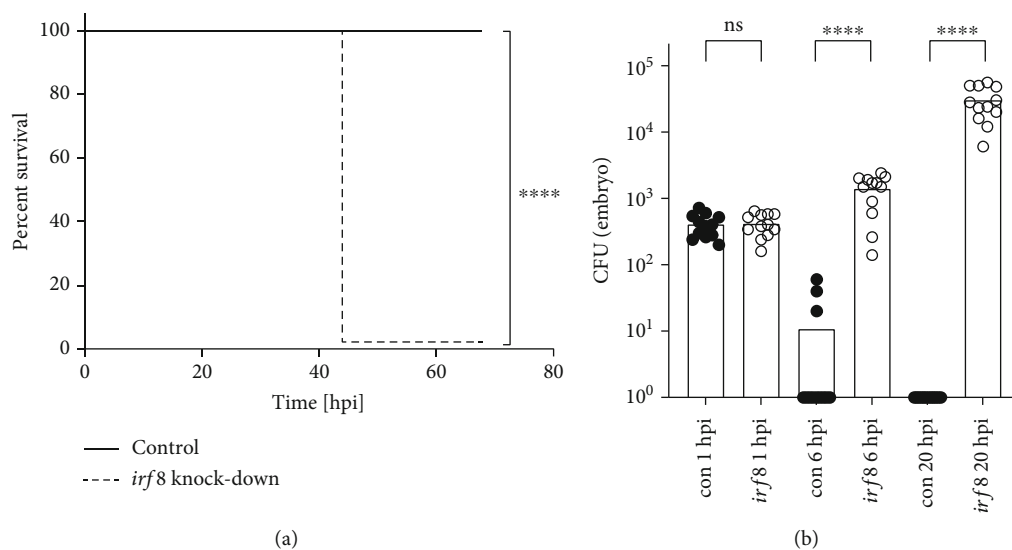


FIGURE 3: Macrophage depletion leads to hypersusceptibility to pneumococcal infection in zebrafish. (a) Survival of control and *irf8* knockdown zebrafish larvae following infection at 54 hpf with 1500 CFU of unencapsulated *S. pneumoniae* D39 Δcps monitored over 68 h post infection ($n \geq 50$ individual animals over two independent experiments). **** $p < 0.0001$. (b) Numbers of viable colony forming units (CFUs) over time within control and *irf8* zebrafish larvae ($n = 12$ individual animals per group per time point over two independent experiments) infected with 1500 CFU of D39 Δcps . **** $p < 0.0001$, ns: not significant.

we knocked down *atp6v0ca* (ATPase H⁺ transporting V0 subunit ca) which encodes one of the subunits of the v-ATPase complex. The efficacy of *atp6v0ca* knockdown was confirmed at the genetic level (Figure S5A). Furthermore, knockdown larvae displayed characteristic pigment dilution (Figure S5B-C) as has been observed in insertional mutants of v-ATPase subunits [37]. It has been previously demonstrated in zebrafish that morpholino-mediated *atp6v0ca* knockdown results in inhibition of lysosomal acidification [38]. Likewise, our CRISPR-mediated knockdown approach led to impaired acidification of internalised pneumococci (Figure S6). In a similar way to bafilomycin A1 treatment, internalised pneumococci in the *atp6v0ca* knockdowns showed lower pHrodo Red (Figure S6C) and higher GFP (Figure S6D) fluorescence intensity indicating higher local pH in comparison to control siblings. Subsequently, we showed that both genetically and chemically induced loss of v-ATPase function leads to impaired resistance of zebrafish larvae to unencapsulated pneumococci (Figure 5(a)). In addition, the pneumococcal killing observed in control larvae was completely abrogated in *atp6v0ca* knockdown and bafilomycin-treated larvae which led to subsequent proliferation of bacteria *in vivo* (Figures 5(b) and 5(c)). Taken together, these data demonstrate the importance of the vacuolar ATPase in acidification and subsequent killing of pneumococci internalised by macrophages *in vivo*.

3. Discussion

In this study, we characterised the innate immune response to systemic *Streptococcus pneumoniae* infection in larval zebrafish. Using this *in vivo* model, we have found that initial phagocytosis by macrophages and subsequent acidification

of ingested bacteria are critical steps for efficient killing and clearance of pneumococci during bloodstream infection in a resolving model using unencapsulated *S. pneumoniae*. In addition, this whole-animal infection model allows the study of the complex crosstalk between different immune cells in their natural environment overcoming the limitations of the *in vitro* studies.

Our results reinforce and validate previous findings that capsular polysaccharide is a major pneumococcal virulence factor associated with immune evasion [4], impeding macrophage phagocytosis *in vivo*. Similar observations have been made in other larval zebrafish studies where another pneumococcal strain representing serotype 4 (TIGR4) was used [20]. Here we have observed increased susceptibility to encapsulated *S. pneumoniae* D39 in systemic infection in larval zebrafish is associated with a reduced capability to internalise the capsular pneumococci. It is generally known that pneumococcal capsule blocks access to surface proteins reducing opsonisation as well as inhibiting nonopsonic phagocytosis [8, 26].

The diminished phagocytosis of encapsulated pneumococci observed in this study may also be related to a lack of a functioning adaptive immune system in zebrafish, as this does not develop before 3-4 weeks postfertilisation [39]. Alternatively, it could be mediated by differential effects of intrinsic complement-mediated but not antibody-mediated opsonisation. In fact, it has been shown *in vitro* that opsonisation by serum containing cognate immunoglobulin results in enhanced binding compared to that by serum containing complement but no IgG [5, 7]. Another *in vitro* study has shown that even in the presence of normal human serum, the rate of binding and internalisation of encapsulated pneumococcus (TIGR4) by RAW macrophages is low and significantly lower than its unencapsulated counterpart TIGR4 Δcps [6].

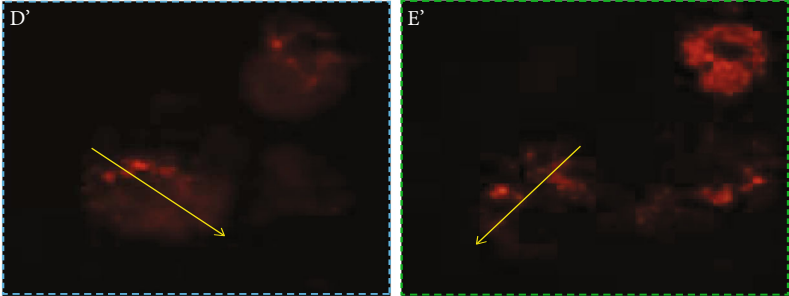
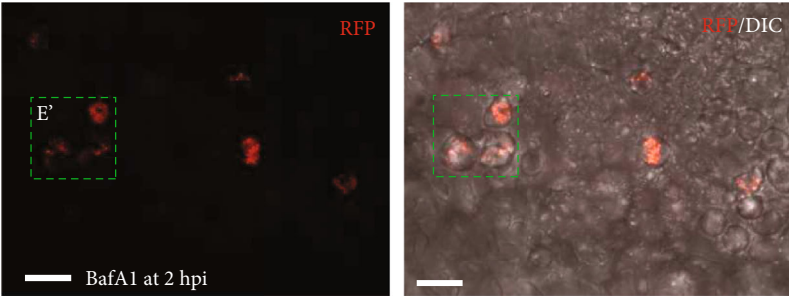
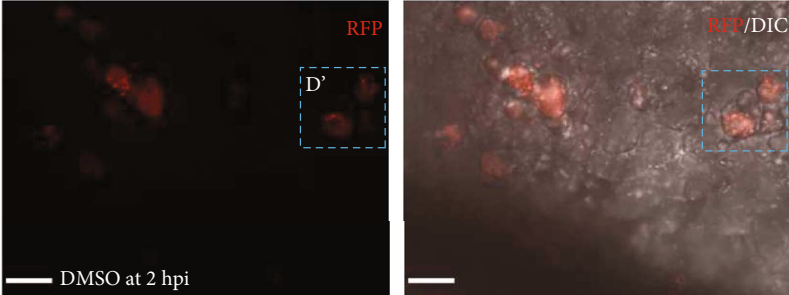
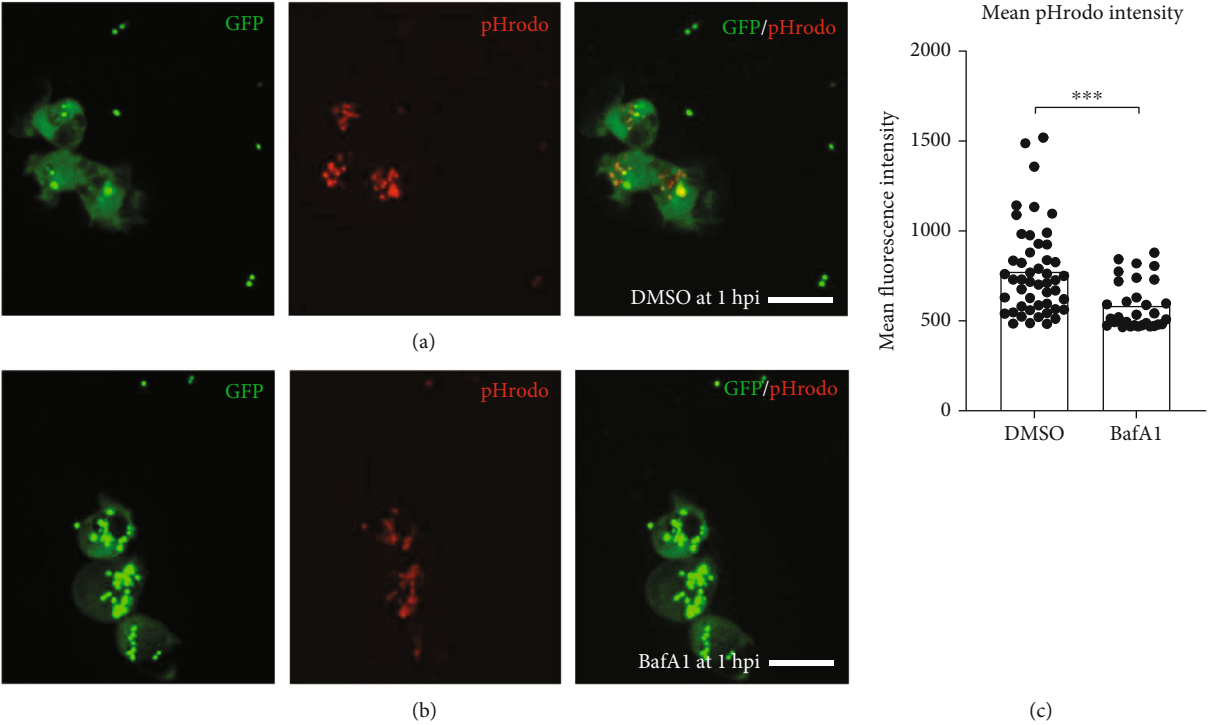


FIGURE 4: Continued.

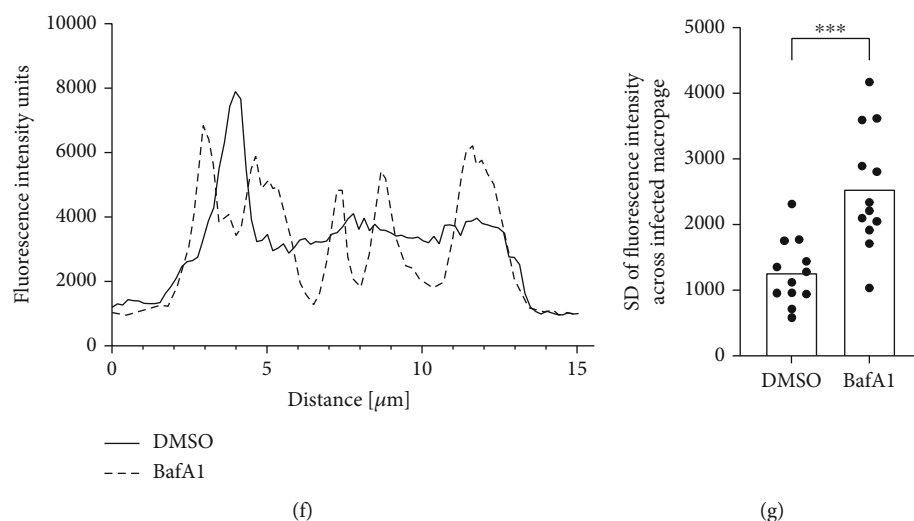


FIGURE 4: A1-mediated inhibition of v-ATPase prevents acidification of macrophage-internalised pneumococci and their subsequent degradation. (a–b) Representative *in vivo* images ($n=5-7$) of circulation valley of *Tg(fms:GFP)* larvae at 1 hpi injected with *S. pneumoniae* D39 Δcps GFP prestained with pHrodo. Panel (a) shows control (DMSO-treated) larvae, whereas panel (b) shows larvae pretreated with 100 nM Bafilomycin A1 (BafA1) at 1 h before infection. (c) Quantification of pHrodo fluorescence intensity within macrophages containing pneumococci ($n=32-49$ phagocytes quantified over 5–7 zebrafish larvae analysed in each group). *** $p < 0.001$. (d–e) Representative *in vivo* images ($n=5-7$) of circulation valley of control (DMSO-treated, d) and bafilomycin A1-treated (e) zebrafish larvae infected with RFP-labelled D39 Δcps . Panels (d') and (e') represent zoomed-in areas from D and E, respectively, where degraded bacteria are present in control macrophages and intact cocci are visible in macrophages of bafilomycin A1-treated zebrafish. (f) Line intensity profiles of the fluorescence signal of *S. pneumoniae*-derived RFP across the yellow arrows shown in (d') and (e'). The signal in a macrophage from bafilomycin A1-treated zebrafish fluctuates across the phagocyte representing the intact internalised pneumococci whereas a control macrophage presents more “averaged” signal across the phagocyte representing intracellular bacterial degradation. (g) Standard deviation of fluorescence intensity values measured across infected macrophages (as shown by arrows in panels (d') and (e')) in DMSO vs. BafA1-treated larvae ($n=12$ infected macrophages within 3 zebrafish larvae were analysed in each group). *** $p < 0.001$. Scale bars represent 15 μm .

Although the unencapsulated pneumococcus is a virulent in our infection model, this lack of pathogenicity was purely due to the activity of zebrafish macrophages, as their depletion led to rapid bacterial proliferation *in vivo* and subsequent death of the infected host. Interestingly, we have shown that even elevated levels of neutrophils in the absence of macrophages are unable to protect the host from systemic pneumococcal infection in this model. Similarly, in the mouse model of infection, macrophages play a vital role in immunity to invading pneumococci and macrophage depletion leads to reduced ability to clear bacteria from both the lung [40] and the bloodstream [41].

Subsequently, we have shown that acidification of macrophage-ingested pneumococci is a key step of host immunity to systemic pneumococcal infection in infected larvae, suggesting bacterial cell death within the macrophage is dependent on v-ATPase-driven acidification of ingested pneumococci. This effect might be indirect, as it is known that low pH is required for activation of lysosomal proteases such as cathepsin D which in turn coordinate microbial killing by macrophages [42, 43]. Furthermore, acidification contributes to degradation of peptidoglycan in Gram positive bacteria, such as *Staphylococcus aureus*, and other microbial pathogen-associated molecular patterns, which in turn are recognised by pattern recognition receptors [44]. This activates production of cytokines and microbicidal factors. Although it is generally accepted that macrophages

kill internalised pneumococci by rapid acidification of bacteria within phagolysosomes [45], to our knowledge this is the first time this has been directly shown *in vivo*. Our model allows direct observation of phagolysosomal maturation associated with bacterial acidification and subsequent bacterial degradation in living vertebrates in real time.

Zebrafish have proven to be a useful platform for drug screening [25] including for anti-infective compounds [46]. The main advantages of this system are the facts that drugs can be simply immersed in zebrafish medium and their effects can be visualised by automated live microscopy. Here, we show that testing for antimicrobials is also feasible in our infection model, by rescuing infected zebrafish larvae with antibiotics supplemented to the medium. In addition, we believe this model can be a useful tool to study the dynamics of antibiotic resistance in pneumococci *in vivo* particularly important in the light of recent emergence of antimicrobial-resistant pneumococci.

In conclusion, we have validated the zebrafish model of systemic pneumococcal infection by demonstrating the importance of pneumococcal capsule and subsequently by revealing the role of macrophages and the acidification of internalised bacteria in resistance to systemic pneumococcal infection. This model is a useful complement to the existing *in vivo* models of pathogen–host interaction in pneumococcal infection.

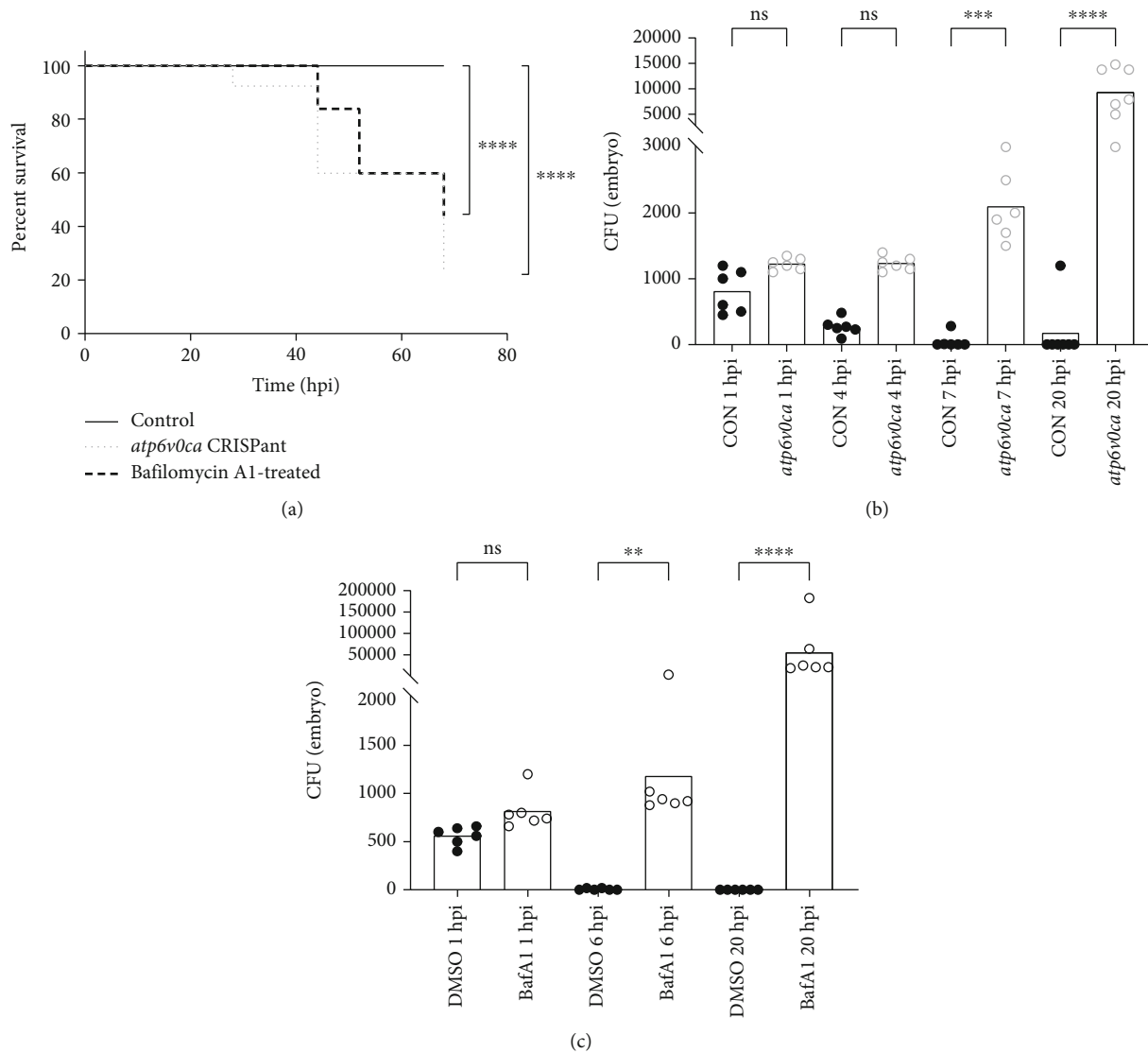


FIGURE 5: Inhibition of v-ATPase leads to hypersusceptibility to pneumococcal infection in zebrafish. (a) Survival of zebrafish control, bafilomycin A1-treated or *atp6v0ca* knockdown larvae following infection with 1500 CFU of unencapsulated *S. pneumoniae* D39 Δcps monitored over 68 h post infection ($n \geq 25$ individual animals over two independent experiments), **** $p < 0.0001$). (b) Numbers of viable colony forming units (CFUs) over time within control and *atp6v0ca* knockdown zebrafish larvae infected with 1500 CFU of D39 Δcps (** $p < 0.001$, **** $p < 0.0001$, ns: not significant). (c) Numbers of viable colony forming units (CFUs) over time within control (DMSO-treated) and bafilomycin A1-treated zebrafish larvae ($n \geq 6$ individual animals per group per time point) infected with 1500 CFU of D39 Δcps (** $p < 0.01$, **** $p < 0.0001$, ns: not significant).

4. Materials and Methods

4.1. Zebrafish Lines and Maintenance. Up to 5 days postfertilisation (dpf), zebrafish are not protected under the Animals (Scientific Procedures) Act 1986. However, all work was carried out according to the stipulations set out in Project License PPL 40/3574. Adult zebrafish were maintained by staff at the University of Sheffield Bateson Centre Zebrafish Facility. Adult fish were kept in a continuous recirculating closed system aquarium with a light/dark cycle of 14/10 hours at 28°C. Larvae were incubated in E3 medium at 28.2°C according to standard protocols [47]. The following zebrafish lines were used in this study: London wild-

type (LWT), *Tg(mpx:GFP)i114* [48], *Tg(mpeg1:mCherry-F)ump2* [49], and *Tg(fms:GFP)sh377* [34].

4.2. Bacterial Culture and Inoculum Preparation. All *Streptococcus pneumoniae* strains (listed in Table 1) were derived from D39 [23] and grown on pre-poured Tryptic Soy Agar 5% sheep blood plates (TSAB 5% SB; Becton Dickinson) at 37°C in an atmosphere containing 5% CO₂. Bacterial cells were grown in Todd-Hewitt Broth (Becton-Dickinson) supplemented with 0.5% yeast extract (BD) at 37°C in an atmosphere containing 5% CO₂ reaching OD₆₀₀ between 0.3 and 0.5. Bacteria were subsequently centrifuged (5000 g, 10 min) and resuspended in phosphate-buffered saline (PBS)

TABLE 1: *S. pneumoniae* strains used in this study.

Strain name	Description/strain genotype	Source/reference
D39	Serotype 2, capsule-positive <i>S. pneumoniae</i> type strain	[23]
D39 Δ <i>cps</i>	Unencapsulated D39 D39 Δ <i>cps</i> (Δ <i>cps2A'</i> - Δ <i>cps2H'</i>)	[23]
'D39 GFP' AKF_Sp0014	GFP-expressing capsule-positive D39 D39 <i>hlpA-gfp_cat</i>	This study [9]
'D39 Δ <i>cps</i> GFP' AKF_Sp0012	GFP-expressing D39 Δ <i>cps</i> D39 Δ <i>cps hlpA-gfp_cat</i>	This study [9]
'D39 Δ <i>cps</i> RFP' AKF_Sp0013	RFP-expressing D39 Δ <i>cps</i> D39 Δ <i>cps hlpA(wt)_hlpA-mKate2_cat</i>	This study [24]

The D39 Δ *cps* genotype (Δ *cps2A'*- Δ *cps2H'*) was excluded from derivative strains for clarity. Transcriptional and translational gene fusions are indicated using an underscore (_) and dash (-), respectively. Cat = chloramphenicol resistance cassette.

supplemented with 2% polyvinylpyrrolidone-40 (PVP40, Sigma-Aldrich).

4.3. Strain Construction. *S. pneumoniae* strains were generated using methods described previously [50]. For all strains, fluorescent constructs were PCR amplified from JWV500 or MK119 gDNA using primers *hlpA_up_F* (AACAAAGTCA GCCACCTGTAG) and *hlpA_down_R* (CGTGGCTGACG ATAATGAGG) before transformation into D39 strain backgrounds [9, 24]. Transformants were selected on TSAII overlay plates containing 5 μ g ml⁻¹ chloramphenicol and confirmed through diagnostic PCR and cytological fluorescence assays.

4.4. pHrodo Red Staining of Pneumococci. The pHrodo Red-succinimidyl ester (Thermo Fisher) was dissolved in DMSO to the final concentration of 2.5 mM. 0.5 μ l of pHrodo Red was added to 200 μ l of bacterial suspension in PBS pH 9 and then mixed thoroughly. The mixture was incubated 30 min at 37°C with gentle rotating. To remove the excess of the dyes, bacteria were washed during 3-step procedure: addition of 1 ml of PBS pH 8, 1 ml of Tris pH 8.5, again 1 ml of PBS pH 8; followed by 2 min of centrifugation in 12000g and gentle removal of the supernatant. After washing, bacterial pellet was resuspended in 200 μ l of PBS pH 7.4 supplemented with 2% PVP40 and proceeded to microinjections of zebrafish larvae.

4.5. Microinjection of Zebrafish Larvae. 54 hpf zebrafish larvae were microinjected into the circulation with bacteria as previously described [51]. Briefly, anaesthetised larvae were embedded in 3% w/v methylcellulose and injected individually with 1 nl using microcapillary pipettes filled with the bacterial suspension of known concentration. Following infection, larvae were observed frequently up to 68 hpf and numbers of dead larvae recorded at each time point.

4.6. TSA Staining. Infected larvae were fixed at 1, 2, and 4 hpi in ice-cold 4% paraformaldehyde in PBS supplemented with 0.5% Triton X-100 (PBS-TX) overnight at 4°C. Subsequently, fixed larvae were washed in PBS-TX three times. Peroxidase activity was detected by incubation in 1:100 Cy5-TSA:amplification reagent (PerkinElmer) in the dark

for 10 min at 28° C followed by extensive washing in PBS-TX.

4.7. Morpholino- and CRISPR/Cas9-Mediated Knockdown. Morpholino-modified antisense oligomers against *irf8* (splice) [28] were injected using a method described previously [32]. Briefly, each embryo was injected with 1 nl of 0.5 mM of *irf8* MO at the 1-4 cell stage. A standard control morpholino (Genetools) was used as a negative control.

For CRISPR/Cas9-mediated *atp6v0ca* (ENSDARG00000 057853) knockdown, the online web tool CHOPCHOP was used to design a gene-specific CRISPR (guide) RNA in exon 3 of the following sequence where PAM site is indicated in brackets: CATTGCCATCTACGGCCTGG (TGG). Synthetic SygRNA (Merck) consisting of gene-specific CRISPR RNA (crRNA) and transactivating RNAs (tracrRNA) in combination with Cas9 nuclease protein (Merck) was used for gene editing. TracrRNA and crRNA were resuspended to a concentration of 50 μ M in nuclease-free water. The gRNA-Cas9 complexes were assembled on ice immediately before injection using a 1:1:1 ratio of crRNA:tracrRNA:Cas9 nuclease with the final concentrations of 16.6 μ M, 16.6 μ M, and 6.6 μ M, respectively. 1 nl of the mixture was injected into each embryo at 1-cell stage. As controls, only Cas9 + tracrRNA were without crRNA. Knockdown verification was performed by the use of primers with the following sequences: forward primer: TCTCTGTTTTTAGCGTTGG GT, reverse primer: ACGCATGACTCACTTGTAGAGC.

4.8. Microscopic Imaging and Analysis. Live anaesthetised larvae were immersed in 1% (w/v) low-melting-point agarose solution in E3 medium and mounted flat on a dish with glass bottom. Images were acquired using a Nikon TE-2000U fluorescence microscope with 4x Nikon Plan Fluor objective (NA 0.13) or UltraVIEW VoX spinning disk confocal microscope (Perkin Elmer) with Olympus 40x UPLFLN oil immersion objective (NA 1.3) or Zeiss LSM 900 Airyscan 2 confocal laser scanning microscope using the C-Apochromat 40x/NA 1.2 water objective. Maximum projections were used for representative images. No nonlinear normalisations were performed. For quantification of pHrodo Red and GFP mean fluorescence intensity, Volocity software (Perkin Elmer) was used.

Bacterial phagocytosis was quantified using an ImageJ custom script called Fish Analysis v5 [52]. All bacteria were identified based on their GFP fluorescence. Subsequently, the fluorescence intensities of the mCherry (macrophage) or Cy5 (neutrophil) channels surrounding ($2\ \mu\text{m}$ radius) the phagocytosed bacteria were measured. The phagocytosed bacteria had high fluorescence mCherry (inside macrophages) or Cy5 (inside neutrophils) intensity of the surrounding area of and the cut-off of 3 times above background level was used to discriminate the phagocytosed from nonphagocytosed bacteria. The areas of bacteria phagocytosed by macrophages, neutrophils, and free in the bloodstream were quantified.

4.9. Determination of In Vivo Bacterial Counts. At various times postinfection, 6–7 living zebrafish larvae were individually transferred with $100\ \mu\text{l}$ of E3 medium into 0.5-ml Precellys tubes containing 1.4-mm ceramic beads (PeqLab) and homogenised using a Precellys 24-Dual homogeniser (PeqLab). The homogenates were serially diluted and spotted on TSA plates containing 5% defibrinated sheep blood to determine *S. pneumoniae* CFU numbers. Bacterial load was also determined for any dead larvae at each time point. The limit of detection was 20 CFU per larva.

4.10. Treatment with Antibiotics. Zebrafish larvae infected with encapsulated D39 pneumococci were bath-treated with a range of concentrations of penicillin G (0.625, 1.25, and $2.5\ \mu\text{g/ml}$, Sigma-Aldrich) or chloramphenicol ($80\ \mu\text{g/ml}$, Sigma-Aldrich) in E3 medium at 1 hpi.

4.11. Bafilomycin A1 Treatment. Zebrafish larvae were bath-treated with 100 nM bafilomycin A1 (Sigma-Aldrich) in E3 medium at 1 hour before infection. For survival experiments, bafilomycin A1 was removed at 4 hpi by replacing the E3 medium. DMSO was used as vehicle control.

4.12. Statistics. GraphPad Prism 8 was used for statistical analysis. Survival curves were analysed with Log rank (Mantel-Cox) test. For pHrodo Red and GFP fluorescence intensity as well as SD of fluorescence intensity, an unpaired *t*-test was performed. For CFU and phagocyte counts as well as bacterial area, a Kruskal-Wallis test was performed using Dunn's multiple comparisons test. Statistical significance was assumed at *P*-values below 0.05.

Data Availability

The data used to support the findings of this study are available from the corresponding author upon request.

Additional Points

Take Aways. (i) Macrophages are essential for pneumococcal killing during zebrafish infection. (ii) Phagosomal acidification is required to kill internalised pneumococci. (iii) The capsule surrounding the pneumococcus protects it from phagocytosis *in vivo*. (iv) Antibiotic treatment effects on the pneumococcus can be studied in zebrafish.

Conflicts of Interest

The authors declare no conflict of interests.

Acknowledgments

We would like to thank the Bateson Centre aquarium staff for zebrafish maintenance and care. This work was supported by the AMR cross-council funding from the MRC to the SHIELD consortium "Optimising Innate Host Defence to Combat Antimicrobial Resistance" MRNO2995X/1 and National Science Centre of Poland under Sonata Bis 9 project (Grant number: 2019/34/E/NZ6/00137). TKP was also funded by Polish National Agency for Academic Exchange under Polish Returns 2019 project (Grant number: PPN/PPO/2019/1/00029/U/0001). AKF and SAR are supported by an MRC New Investigator Research Grant (Grant number: MR/S009280/1).

Supplementary Materials

Figure S1. *S. pneumoniae*-infected zebrafish larvae can be cured by antibiotic treatment. Figure S2. Separate fluorescence channels from Figure 2(b) - encapsulated pneumococci. Figure S3. Separate fluorescence channels from Figure 2(b) - unencapsulated pneumococci. Figure S4. Functional verification of *irf8* knockdown efficiency. Figure S5. Genetic and functional verification of *atp6v0ca* knockdown efficiency. Figure S6. Knockdown of *atp6v0ca* leads to impaired acidification of internalised pneumococci. (*Supplementary Materials*)

References

- [1] B. Henriques-Normark and E. I. Tuomanen, "The pneumococcus: Epidemiology, microbiology, and pathogenesis," *Cold Spring Harbor Perspectives in Medicine*, vol. 3, no. 7, 2013.
- [2] T. van der Poll and S. M. Opal, "Pathogenesis, treatment, and prevention of pneumococcal pneumonia," *The Lancet*, vol. 374, no. 9700, pp. 1543–1556, 2009.
- [3] J. D. Aberdein, J. Cole, M. A. Bewley, H. M. Marriott, and D. H. Dockrell, "Alveolar macrophages in pulmonary host defence: the unrecognized role of apoptosis as a mechanism of intracellular bacterial killing," *Clinical and Experimental Immunology*, vol. 174, no. 2, pp. 193–202, 2013.
- [4] S. Jonsson, D. M. Musher, A. Chapman, A. Goree, and E. C. Lawrence, "Phagocytosis and killing of common bacterial pathogens of the lung by human alveolar macrophages," *Journal of Infectious Diseases*, vol. 152, no. 1, pp. 4–13, 1985.
- [5] F. Ali, M. E. Lee, F. Iannelli et al., "Streptococcus pneumoniae-associated human macrophage apoptosis after bacterial internalization via complement and Fcγ receptors correlates with intracellular bacterial load," *Journal of Infectious Diseases*, vol. 188, no. 8, pp. 1119–1131, 2003.
- [6] J. Ercoli, G. Ercoli, T. Pollard et al., "Relative contributions of extracellular and internalized bacteria to early macrophage proinflammatory responses to streptococcus pneumoniae," *MBio*, vol. 10, no. 5, 2019.
- [7] S. B. Gordon, G. R. B. Irving, R. A. Lawson, M. E. Lee, and R. C. Read, "Intracellular trafficking and killing of Streptococcus pneumoniae by human alveolar macrophages are influenced

- by opsonins," *Infection and Immunity*, vol. 68, no. 4, pp. 2286–2293, 2000.
- [8] C. Hyams, E. Camberlein, J. M. Cohen, K. Bax, and J. S. Brown, "The *Streptococcus pneumoniae* capsule inhibits complement activity and neutrophil phagocytosis by multiple mechanisms," *Infection and Immunity*, vol. 78, no. 2, pp. 704–715, 2010.
- [9] M. Kjos, R. Aprianto, V. E. Fernandes et al., "Bright fluorescent *Streptococcus pneumoniae* for live-cell imaging of host-pathogen interactions," *Journal of Bacteriology*, vol. 197, no. 5, pp. 807–818, 2015.
- [10] G. Ercoli, V. E. Fernandes, W. Y. Chung et al., "Intracellular replication of *Streptococcus pneumoniae* inside splenic macrophages serves as a reservoir for septicemia," *Nature Microbiology*, vol. 3, no. 5, pp. 600–610, 2018.
- [11] M. V. Surve, S. Bhutda, A. Datey et al., "Heterogeneity in pneumolysin expression governs the fate of *Streptococcus pneumoniae* during blood-brain barrier trafficking," *PLoS Pathogens*, vol. 14, no. 7, article e1007168, 2018.
- [12] P. Elsbach and J. Weiss, "Oxygen-dependent and oxygen-independent mechanisms of microbicidal activity of neutrophils," *Immunology Letters*, vol. 11, no. 3–4, pp. 159–163, 1985.
- [13] H. M. Marriott, L. E. Jackson, T. S. Wilkinson et al., "Reactive oxygen species regulate neutrophil recruitment and survival in pneumococcal pneumonia," *American Journal of Respiratory and Critical Care Medicine*, vol. 177, no. 8, pp. 887–895, 2008.
- [14] J. A. Preston, M. A. Bewley, H. M. Marriott et al., "Alveolar macrophage apoptosis-associated bacterial killing helps prevent murine pneumonia," *American Journal of Respiratory and Critical Care Medicine*, vol. 200, no. 1, pp. 84–97, 2019.
- [15] G. L. Lukacs, O. D. Rotstein, and S. Grinstein, "Phagosomal acidification is mediated by a vacuolar-type H(+)-ATPase in murine macrophages," *Journal of Biological Chemistry*, vol. 265, no. 34, pp. 21099–21107, 1990.
- [16] M. E. Maxson and S. Grinstein, "The vacuolar-type H⁺-ATPase at a glance - more than a proton pump," *Journal of Cell Science*, vol. 127, no. 23, pp. 4987–4993, 2014.
- [17] J. Westman and S. Grinstein, "Determinants of phagosomal pH during host-pathogen interactions," *Frontiers in Cell and Developmental Biology*, vol. 8, 2020.
- [18] K. Watson, C. D. Russell, J. K. Baillie et al., "Developing novel host-based therapies targeting microbicidal responses in macrophages and neutrophils to combat bacterial antimicrobial resistance," *Frontiers in Immunology*, vol. 11, p. 786, 2020.
- [19] M. C. Gomes and S. Mostowy, "The case for modeling human infection in zebrafish," *Trends in Microbiology*, vol. 28, no. 1, pp. 10–18, 2020.
- [20] S. Rounioja, A. Saralahti, L. Rantala et al., "Defense of zebrafish embryos against *Streptococcus pneumoniae* infection is dependent on the phagocytic activity of leukocytes," *Developmental and Comparative Immunology*, vol. 36, no. 2, pp. 342–348, 2012.
- [21] K. K. Jim, J. Y. Engelen-Lee, A. M. van der Sar et al., "Infection of zebrafish embryos with live fluorescent *Streptococcus pneumoniae* as a real-time pneumococcal meningitis model," *Journal of Neuroinflammation*, vol. 13, no. 1, p. 188, 2016.
- [22] A. Saralahti and M. Rämetsä, "Zebrafish and streptococcal infections," *Scandinavian Journal of Immunology*, vol. 82, no. 3, pp. 174–183, 2015.
- [23] J. A. Lanie, W. L. Ng, K. M. Kazmierczak et al., "Genome sequence of Avery's virulent serotype 2 strain D39 of *Streptococcus pneumoniae* and comparison with that of unencapsulated laboratory strain R6," *Journal of Bacteriology*, vol. 189, no. 1, pp. 38–51, 2007.
- [24] M. Kjos and J. W. Veening, "Tracking of chromosome dynamics in live *Streptococcus pneumoniae* reveals that transcription promotes chromosome segregation," *Molecular Microbiology*, vol. 91, no. 6, pp. 1088–1105, 2014.
- [25] A. J. Rennekamp and R. T. Peterson, "15 years of zebrafish chemical screening," vol. 24, pp. 58–70, 2015.
- [26] A. Kadioglu, J. N. Weiser, J. C. Paton, and P. W. Andrew, "The role of *Streptococcus pneumoniae* virulence factors in host respiratory colonization and disease," *Nature Reviews Microbiology*, vol. 6, no. 4, pp. 288–301, 2008.
- [27] D. Shi, G. Mi, M. Wang, and T. J. Webster, "In vitro and ex vivo systems at the forefront of infection modeling and drug discovery," *Biomaterials*, vol. 198, pp. 228–249, 2019.
- [28] L. Li, H. Jin, J. Xu, Y. Shi, and Z. Wen, "Irf8 regulates macrophage versus neutrophil fate during zebrafish primitive myelopoiesis," *Blood*, vol. 117, no. 4, pp. 1359–1369, 2011.
- [29] F. Ellett, V. Pazhakh, L. Pase et al., "Macrophages protect *Talaromyces marneffe* conidia from myeloperoxidase-dependent neutrophil fungicidal activity during infection establishment in vivo," *PLoS Pathogens*, vol. 14, no. 6, p. e1007063, 2018.
- [30] S. Masud, T. K. Prajsnar, V. Torraca et al., "Macrophages target *Salmonella* by Lc3-associated phagocytosis in a systemic infection model," *Autophagy*, vol. 15, no. 5, pp. 796–812, 2019.
- [31] A. J. Pagan, C. T. Yang, J. Cameron et al., "Myeloid growth factors promote resistance to mycobacterial infection by curtailing granuloma necrosis through macrophage replenishment," *Cell Host and Microbe*, vol. 18, no. 1, pp. 15–26, 2015.
- [32] T. K. Prajsnar, R. Hamilton, J. Garcia-Lara et al., "A privileged intraphagocyte niche is responsible for disseminated infection of *Staphylococcus aureus* in a zebrafish model," *Cellular Microbiology*, vol. 14, no. 10, pp. 1600–1619, 2012.
- [33] A. Yamamoto, Y. Tagawa, T. Yoshimori, Y. Moriyama, R. Masaki, and Y. Tashiro, "Bafilomycin A1 prevents maturation of autophagic vacuoles by inhibiting fusion between autophagosomes and lysosomes in rat hepatoma cell line, H-4-II-E cells," *Cell Structure and Function*, vol. 23, no. 1, pp. 33–42, 1998.
- [34] C. T. Dee, R. T. Nagaraju, E. I. Athanasiadis et al., "CD4-transgenic zebrafish reveal tissue-resident Th2- and regulatory T cell-like populations and diverse mononuclear phagocytes," *The Journal of Immunology*, vol. 197, no. 9, pp. 3520–3530, 2016.
- [35] T. K. Prajsnar, J. J. Serba, B. M. Dekker et al., "The autophagic response to *Staphylococcus aureus* provides an intracellular niche in neutrophils," *Autophagy*, vol. 17, no. 4, pp. 888–902, 2021.
- [36] N. C. Shaner, G. H. Patterson, and M. W. Davidson, "Advances in fluorescent protein technology," *Journal of Cell Science*, vol. 120, no. 24, pp. 4247–4260, 2007.
- [37] J. L. Ramos-Balderas, S. Carrillo-Rosas, A. Guzman, R. E. Navarro, and E. Maldonado, "The zebrafish mutants for the V-ATPase subunits d, ac 45, E, H and c and their variable pigment dilution phenotype," *BMC Research Notes*, vol. 6, no. 1, pp. 1–9, 2013.
- [38] T. Sasaki, S. Lian, A. Khan et al., "Autolysosome biogenesis and developmental senescence are regulated by both Spn1 and v-ATPase," *Autophagy*, vol. 13, no. 2, pp. 386–403, 2017.

- [39] C. E. Willett, A. Cortes, A. Zuasti, and A. G. Zapata, "Early hematopoiesis and developing lymphoid organs in the zebrafish," *Developmental Dynamics*, vol. 214, no. 4, pp. 323–336, 1999.
- [40] D. H. Dockrell, H. M. Marriott, L. R. Prince et al., "Alveolar macrophage apoptosis contributes to pneumococcal clearance in a resolving model of pulmonary infection," *The Journal of Immunology*, vol. 171, no. 10, pp. 5380–5388, 2003.
- [41] A. Gerlini, L. Colomba, L. Furi et al., "The role of host and microbial factors in the pathogenesis of pneumococcal bacteraemia arising from a single bacterial cell bottleneck," *PLoS Pathogens*, vol. 10, no. 3, p. e1004026, 2014.
- [42] M. A. Bewley, H. M. Marriott, C. Tulone et al., "A cardinal role for cathepsin D in co-ordinating the host-mediated apoptosis of macrophages and killing of pneumococci," *PLoS Pathogens*, vol. 7, no. 1, article e1001262, 2011.
- [43] M. A. Bewley, M. Naughton, J. Preston et al., "Pneumolysin activates macrophage lysosomal membrane permeabilization and executes apoptosis by distinct mechanisms without membrane pore formation," *MBio*, vol. 5, no. 5, pp. e01710–e01714, 2014.
- [44] A. J. Wolf, A. Arruda, C. N. Reyes et al., "Phagosomal degradation increases TLR access to bacterial ligands and enhances macrophage sensitivity to bacteria," *The Journal of Immunology*, vol. 187, no. 11, pp. 6002–6010, 2011.
- [45] J. Cole, J. Aberdein, J. Jubrail, and D. H. Dockrell, "The Role of Macrophages in the Innate Immune Response to *Streptococcus pneumoniae* and *Staphylococcus aureus*," *Mechanisms and Contrasts. In Advances in Microbial Physiology*, vol. 65, pp. 125–202, 2014.
- [46] A. Ordas, R. J. Raterink, F. Cunningham et al., "Testing tuberculosis drug efficacy in a zebrafish high-throughput translational medicine screen," *Antimicrobial Agents and Chemotherapy*, vol. 59, no. 2, pp. 753–762, 2015.
- [47] C. Nüsslein-Volhard and R. Dham, *Zebrafish: a practical approach*, Oxford University Press, New York, 2003.
- [48] S. A. Renshaw, C. A. Loynes, D. M. I. Trushell, S. Elworthy, P. W. Ingham, and M. K. B. Whyte, "A transgenic zebrafish model of neutrophilic inflammation," *Blood*, vol. 108, no. 13, pp. 3976–3978, 2006.
- [49] A. Bernut, J. L. Herrmann, K. Kissa et al., "Mycobacterium abscessus cording prevents phagocytosis and promotes abscess formation," *Proceedings of the National Academy of Sciences of the United States of America*, vol. 111, no. 10, pp. E943–E952, 2014.
- [50] A. K. Fenton, L. MortajiEl, D. T. C. Lau, D. Z. Rudner, and T. G. Bernhardt, "CozE is a member of the MreCD complex that directs cell elongation in *Streptococcus pneumoniae*," *Nature Microbiology*, vol. 2, 2017.
- [51] T. K. Prajsnar, V. T. Cunliffe, S. J. Foster, and S. A. Renshaw, "A novel vertebrate model of *Staphylococcus aureus* infection reveals phagocyte-dependent resistance of zebrafish to non-host specialized pathogens," *Cellular Microbiology*, vol. 10, no. 11, pp. 2312–2325, 2008.
- [52] B. Salamaga, T. K. Prajsnar, A. Jareño-Martinez et al., "Bacterial size matters: multiple mechanisms controlling septum cleavage and diplococcus formation are critical for the virulence of the opportunistic pathogen *Enterococcus faecalis*," *PLoS Pathogens*, vol. 13, no. 7, p. e1006526, 2017.